

## 152. Selectivity of Intramolecular Radical Addition Reactions Cyclization of $\omega$ -Alkenyl Radicals

by Peter Bischof

Institut für Organische Chemie der Universität Heidelberg, D-6900 Heidelberg

(2.VI.80)

---

### Summary

Small  $\omega$ -alkenyl radicals are known to cyclize exclusively *via* the unexpected *Anti-Markownikow* pathway which leads to cycloalkyl-methyl radicals as the observed reaction products. The strong kinetic preference diminishes, as the linking methylene chain becomes larger. Semiempirical calculations using MINDO/3-UHF allow to classify the observed reaction pathways as individual probes between allowed ( $n=1$ , route **A**) and electronically favourable ( $n=\infty$ , route **M**) routes of reactions.

---

**Introduction.** – The reactivity and selectivity of radicals toward double bonds still represents a world of facts worthwhile to be explored. Literally thousands of experimental data have been collected in the last few decades, some of which are still waiting to be explained.

The troubles the experimentalist faces to interpret his results in terms of elementary reactions are mainly due to two circumstances: Firstly, the reactants are in fact intermediates in a series of reaction steps and secondly, there is in most cases a wide manifold of competing reaction pathways which contaminate the data obtained by experiment. In other words: Individual elementary reaction steps are very hard to be unambiguously verified by such methods.

An elegant way out of the jumble, therefore, seems to be given by '*Experimental Computer Chemistry*' [1] where any individual reaction step can be simulated. In order to go this way properly, one has to choose a procedure reasonably cheap and still reliable enough to reproduce and/or predict experimental facts.

MINDO/3 [2]-UHF [3] has indicated [4–8] to be a surprisingly useful tool for this purpose. We have applied this method to a large number of intramolecular radical addition reactions and wish to discuss the obtained results in this work.

The attack of a double bond by an alkyl radical is a rapid process involving usually a low activation barrier of about 24 kJ/mol [5]. If the double bond is non-symmetrically substituted, the attack can in principle lead to either the

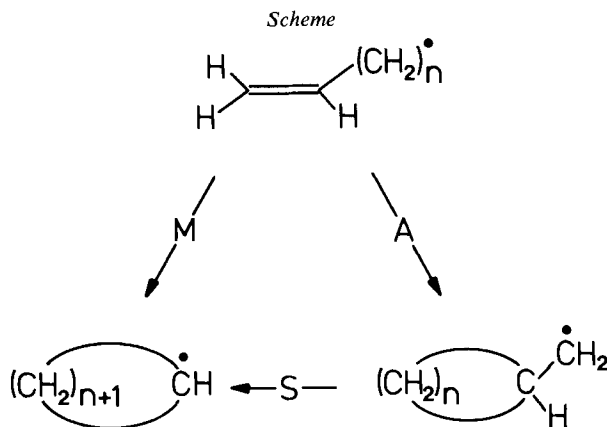
thermodynamically more stable or less stable product radical. The former pathway has been named [8] the *Markownikow* route **M**, the latter accordingly the *Anti-Markownikow* route **A**. Theory predicts [5] that in case of a bimolecular reaction, route **M** is favoured by a lower activation energy thus leading to the 'natural', more stable product. We wish to emphasize, that this coincidence, at first sight being obvious, is in fact rather surprising. It is well known, that alkanes are more stable, the more branched they are<sup>1)</sup>; hence, two geminal methyl groups should have a net attractive interaction energy. In contrast to this expectation, the calculations [5] trace the higher activation energy for route **A** in the addition of methyl to propene to be due to the repulsion between the two methyl groups.

Experiment supports this result: The addition of methyl is faster, the less alkylated the double bond is [10]. The tendency of radicals to add in bimolecular reactions according to route **M** is therefore a consequence of electronic [11] and steric effects adding up to the same trend.

The situation becomes very interesting, if the double bond and the radical center are part of the same molecule. In this case, the formerly bimolecular addition turns into a radical cyclization reaction. The parent system consists of an inert methylene chain linking the two reaction sites together. This is illustrated in the *Scheme*.

Knowing that the intermolecular radical addition is - as indicated above - a very rapid process, it is not surprising, that its intramolecular counterpart (*i.e.* the  $\omega$ -alkenyl radical cyclization) is indeed the most oftenly observed radical rearrangement. However, the fact, that in most cases these rearrangement take the alternative *Anti-Markownikow* pathway adds further interest to their study. We have therefore decided to explore the associated potential energy surfaces of the parent systems by means of MINDO/3-UHF calculations. The smallest member of the series has already been investigated within this model [6].

As indicated in the *Scheme*, there will be three types of reactants to be considered in this context: 1)  $\omega$ -alkenyl radicals (**n**), 2) cycloalkyl radicals (**nM**)



<sup>1)</sup> The reader may compare the experimental values in [9].

and 3) cycloalkyl-methyl radicals (**nA**). In the next paragraphs, we shall discuss the calculated structures and properties of these reactants in detail. The obtained thermodynamical data are summarized in *Table 1*.

Table 1. Heats of formation  $\Delta H_f$ , hydrogen atom affinities  $\Delta H_H$  and standard entropies  $S_{298}^0$  of  $\omega$ -alkenyl radicals (**n**), cycloalkyl radicals (**nM**) and cycloalkyl-methyl radicals (**nA**) calculated by MINDO/3. All values in kJ/mol and J/Kmol respectively

n	2	3	4	5
$\Delta H_f$ ( <b>n</b> )	158	130	104	78
$\Delta H_H$ ( <b>n</b> )	378	377	377	377
$S_{298}^0$ ( <b>n</b> ) <sup>a)</sup>	324	364	403	443
$\Delta H_f$ ( <b>nM</b> )	112	11	-37	-62
$\Delta H_H$ ( <b>nM</b> )	351	345	334	328
$S_{298}^0$ ( <b>nM</b> ) <sup>a)</sup>	281	303	332	356
$\Delta H_f$ ( <b>nA</b> )	159	110	38	8
$\Delta H_H$ ( <b>nA</b> )	369	372	376	370
$S_{298}^0$ ( <b>nA</b> ) <sup>a)</sup>	294	321	346	363

<sup>a)</sup> See appendix B.

**$\omega$ -Alkenyl Radicals.** – These open chain reactants can assume various stable conformations which all correspond to local minima on the potential energy surfaces. If *n* is the number of methylene groups (as defined in the *Scheme*), there is a total number of  $3^n$  rotamers being expected, each of which might be the one of lowest energy.

This expected ‘hilly’ behaviour of the potential energy surfaces is bound to complicate the location of the equilibrium structure tremendously, since any calculation will converge to the one rotamer minimum closest to the starting point. Fortunately, a large number of them could be omitted for geometrical reasons and the aid of *Dreiding* models helped us to reduce the number of necessary optimization runs to a reasonable amount.

The results of all these calculations can be summarized as follows: The most stable structure of any  $\omega$ -alkenyl radical consists of an all *trans*-methylene-chain which substitutes the terminal double bond in *gauche* conformation. The optimized structures of the calculated 3-butenyl radical (**2**), 4-pentenyl radical (**3**), 5-hexenyl radical (**4**) and 6-heptenyl radical (**5**) are shown in *Figure 1*, the relevant structural data have been collected in *Table 2*.

Although the energy differences between the various rotamers are small (generally below 2 kJ/mol), their calculated main moments of inertia and thus their standard entropies<sup>2)</sup> are very much depending on the conformation of lowest energy.

Apart from this conformational identity within the series of homologue  $\omega$ -alkenyl radicals, there are some other aspects which are important to understand the observed and predicted reactivities and selectivities of  $\omega$ -alkenyl radicals. For this discussion, it is convenient to name the ‘radical orbital’ in a localized picture

<sup>2)</sup> Calculated according to [12].

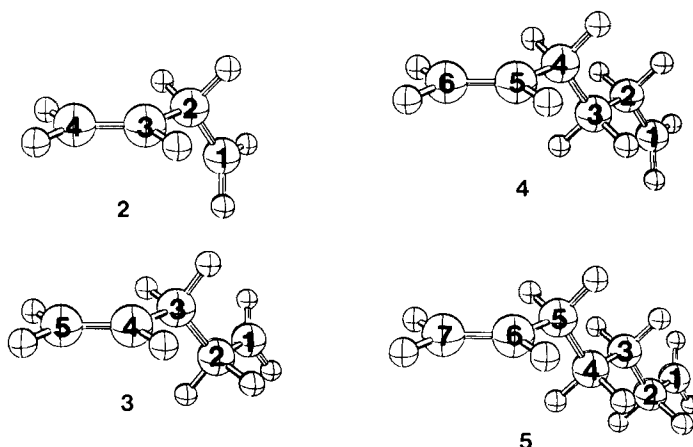


Fig. 1. Calculated structures of lowest energy of the  $\omega$ -alkenyl radicals  $n$ . The numbering given is used to define the structural data summarized in Table 2.

as  $\rho$ . Hence,  $\rho$  is a single p orbital if the radical center is planar and a  $sp^x$ -hybrid orbital if the radical is pyramidal.

The structural influence of a radical center as compared to the parent hydrocarbon can then be understood by the effects due to the conjugation of  $\rho$  with other orbitals of the molecule.

It is wellknown, that methylene groups are associated with high lying *pseudo*  $\pi$ -orbitals which offer a possibility to conjugate with other orbitals such as  $\rho$ . This interaction is qualitatively illustrated in Figure 2. In alkyl and alkenyl radicals this conjugation should lead to the following consequences:

1) Since the interacting two orbitals contain three electrons only, the conjugation is stabilizing. This stabilization 'locks' the radical center into the conformation where the conjugation reaches its maximum and which has been obtained for all structures shown in Figure 1. Note, that although the resulting stabilization energy might be minute, ESR. studies fully establish the importance of its influence to the conformation<sup>3)</sup> [13a];

2) The conjugation adds some  $\pi$ -character to the C,C-bond which results in a marked shortening of its length;

3) The methylene group (as the two electron contributor) this way loses part of its binding electron density thus lengthening the C,H-bonds;

4) This density is added to  $\rho$  which increases the negative charge at the radical center. This charge drift leads to structural change at the radical center C(1) in such a way, that the radical is more pyramidal, the larger the negative charge at C(1) is. Surprisingly, this charge drift into the radical center is most pronounced in the case of 3 and slowly diminishes with increasing length of the methylene chain.

<sup>3)</sup> It should be noted, that the predicted reactant structures are in full agreement with experiment (see [13]).

Table 2. Symmetries and structural parameters of equilibrium structures **n**, **nA**, **nM** and activated complexes **nT<sub>A</sub>**, **nT<sub>M</sub>** and **nT<sub>S</sub>**. Bond lengths (CC resp. CH) in Å, bond angles (CCC) and dihedral angles (CCCC) in degrees. Full tables of cartesian coordinates are available upon request.

<b>2</b>	$C_I$	C(1), C(2) 1.454, C(2), C(3) 1.489, C(3), C(4) 1.327, C(1), H 1.096, C(2), H 1.125, C(3), H 1.112, C(4), H 1.100, C(1), C(2), C(3) 120, C(2), C(3), C(4) 132, C(1), C(2), C(3), C(4) 110;
<b>3</b>	$C_I$	C(1), C(2) 1.454, C(2), C(3) 1.513, C(3), C(4) 1.490, C(4), C(5) 1.327, C(1), H 1.096, C(2), H 1.125, C(3), H 1.122, C(4), H 1.113, C(5), H 1.100, C(1), C(2), C(3) 121, C(2), C(3), C(4) 120, C(3), C(4), C(5) 132, C(1), C(2), C(3), C(4) 179, C(2), C(3), C(4), C(5) 118;
<b>4</b>	$C_I$	C(1), C(2) 1.454, C(2), C(3) 1.514, C(3), C(4) 1.515, C(4), C(5) 1.491, C(5), C(6) 1.327, C(1), H 1.096, C(2), H 1.125, C(3), H 1.122, C(4), H 1.122, C(5), H 1.113, C(6), H 1.100, C(1), C(2), C(3) 121, C(2), C(3), C(4) 120, C(3), C(4), C(5) 119, C(4), C(5), C(6) 132, C(1), C(2), C(3), C(4) 180, C(2), C(3), C(4), C(5) 179, C(3), C(4), C(5), C(6) 110;
<b>5</b>	$C_I$	C(1), C(2) 1.454, C(2), C(3) 1.514, C(3), C(4) 1.515, C(4), C(5) 1.515, C(5), C(6) 1.491, C(6), C(7) 1.328, C(1), H 1.096, C(2), H 1.125, C(3), H 1.122, C(4), H 1.122, C(5), H 1.122, C(6), H 1.113, C(7), H 1.100, C(1), C(2), C(3) 121, C(2), C(3), C(4) 120, C(3), C(4), C(5) 120, C(4), C(5), C(6) 119, C(5), C(6), C(7) 132, C(1), C(2), C(3), C(4) 180, C(2), C(3), C(4), C(5) 180, C(3), C(4), C(5), C(6) 179, C(4), C(5), C(6), C(7) 110;
<b>2A</b>	$C_I$	C(1), C(2) 1.440, C(2), C(3) 1.522, C(3), C(4) 1.480, C(2), C(4) 1.526, C(1), H 1.096, C(2), H 1.118, C(3), H 1.106, C(4), H 1.106, C(1), C(2), C(3) 127, C(1), C(2), C(4) 127, C(3), C(2), C(4) 58, C(1), C(2), C(3), C(4) 115;
<b>3A</b>	$C_s$	C(1), C(2) 1.461, C(2), C(3) 1.545, C(3), C(4) 1.522, C(1), H 1.096, C(2), H 1.130, C(3), H 1.114, C(4), H 1.113, C(1), C(2), C(3) 123, C(2), C(3), C(4) 91, C(3), C(4), C(5) 90, C(1), C(2), C(3), C(4) 130, C(2), C(3), C(4), C(5) 0;
<b>4A</b>	$C_s$	C(1), C(2) 1.467, C(2), C(3) 1.546, C(3), C(4) 1.524, C(4), C(5) 1.523, C(1), H 1.097, C(2), H 1.135, C(3), H 1.117, C(4), H 1.116, C(1), C(2), C(3) 118, C(2), C(3), C(4) 109, C(3), C(4), C(5) 108, C(6), C(2), C(3) 105, C(1), C(2), C(3), C(4) 142, C(2), C(3), C(4), C(5) 5;
<b>5A</b>	$C_s$	C(1), C(2) 1.473, C(2), C(3) 1.540, C(3), C(4) 1.519, C(4), C(5) 1.518, C(1), H 1.096, C(2), H 1.138, C(3), H 1.120, C(4), H 1.120, C(5), H 1.120, C(1), C(2), C(3) 115, C(2), C(3), C(4) 118, C(3), C(4), C(5) 117, C(4), C(5), C(6) 116, C(3), C(2), C(7) 113, C(1), C(2), C(3), C(4) 186, C(2), C(3), C(4), C(5) 37, C(3), C(4), C(5), C(6) – 33, C(7), C(2), C(3), C(4) – 38;
<b>2M</b>	$C_{2v}$	C(1), C(2) 1.486, C(2), C(3) 1.531, C(1), H 1.095, C(2), H 1.115, C(3), H 1.114, C(1), C(2), C(3) 88, C(2), C(3), C(4) 90, C(2), C(1), C(4) 94;
<b>3M</b>	$C_{2v}$	C(1), C(2) 1.484, C(2), C(3) 1.526, C(3), C(4) 1.530, C(1), H 1.098, C(2), H 1.119, C(3), H 1.116, C(1), C(2), C(3) 106, C(2), C(3), C(4) 108, C(2), C(1), C(5) 112;
<b>4M</b>	$C_s$	C(1), C(2) 1.480, C(2), C(3) 1.520, C(3), C(4) 1.520, C(1), H 1.103, C(2), H 1.122, C(3), H 1.119, C(4), H 1.120, C(1), C(2), C(3) 116, C(2), C(3), C(4) 117, C(3), C(4), C(5) 117, C(2), C(1), C(6) 124, C(1), C(2), C(3), C(4) 26, C(2), C(3), C(4), C(5) – 35, C(3), C(2), C(1), C(6) – 19;
<b>5M</b>	$C_2$	C(1), C(2) 1.476, C(2), C(3) 1.516, C(3), C(4) 1.517, C(4), C(5) 1.517, C(1), H 1.106, C(2), H 1.124, C(3), H 1.120, C(4), H 1.120, C(1), C(2), C(3) 122, C(2), C(3), C(4) 121, C(3), C(4), C(5) 121, C(2), C(1), C(7) 131, C(1), C(2), C(3), C(4) 45, C(2), C(3), C(4), C(5) – 60, C(3), C(4), C(5), C(6) 55, C(6), C(7), C(1), C(2) – 38;
<b>2T<sub>A</sub></b>	$C_I$	C(1), C(2) 1.452, C(2), C(3) 1.492, C(3), C(4) 1.362, C(1), H 1.100, C(2), H 1.112, C(3), H 1.114, C(4), H 1.098, C(1), C(2), C(3) 81, C(2), C(3), C(4) 132, C(1), C(2), C(3), C(4) 101; $\alpha$ (= C(1), C(3)) 1.913;

- 3T<sub>A</sub>**  $C_I$  C(1), C(2) 1.481, C(2), C(3) 1.516, C(3), C(4) 1.509, C(4), C(5) 1.361, C(1), H 1.104, C(2), H 1.116, C(3), H 1.117, C(4), H 1.115, C(5), H 1.099, C(1), C(2), C(3) 98, C(2), C(3), C(4) 103, C(3), C(4), C(5) 131, C(1), C(2), C(3), C(4) 3, C(2), C(3), C(4), C(5) - 114;  $a$  (= C(1), C(4)) 2.076;
- 4T<sub>A</sub>**  $C_I$  C(1), C(2) 1.478, C(2), C(3) 1.520, C(3), C(4) 1.519, C(4), C(5) 1.502, C(5), C(6) 1.357, C(1), H 1.104, C(2), H 1.119, C(3), H 1.119, C(4), H 1.119, C(5), H 1.115, C(6), H 1.099, C(1), C(2), C(3) 113, C(2), C(3), C(4) 115, C(3), C(4), C(5) 116, C(4), C(5), C(6) 129, C(1), C(2), C(3), C(4) - 11, C(2), C(3), C(4), C(5) 19, C(3), C(4), C(5), C(6) - 131;  $a$  (= C(1), C(5)) 2.200;
- 5T<sub>A</sub>**  $C_I$  C(1), C(2) 1.477, C(2), C(3) 1.516, C(3), C(4) 1.516, C(4), C(5) 1.517, C(5), C(6) 1.505, C(6), C(7) 1.361, C(1), H 1.105, C(2), H 1.122, C(3), H 1.120, C(4), H 1.120, C(5), H 1.121, C(6), H 1.114, C(7), H 1.099, C(1), C(2), C(3) 118, C(2), C(3), C(4) 119, C(3), C(4), C(5) 119, C(4), C(5), C(6) 121, C(5), C(6), C(7) 128, C(1), C(2), C(3), C(4) 45, C(2), C(3), C(4), C(5) - 48, C(3), C(4), C(5), C(6) 51, C(4), C(5), C(6), C(7) 80;  $a$  (= C(1), C(6)) 2.200;
- 2T<sub>M</sub>**  $C_I$  C(1), C(2) 1.488, C(2), C(3) 1.489, C(3), C(4) 1.377, C(1), H 1.105, C(2), H 1.115, C(3), H 1.105, C(4), H 1.105, C(1), C(2), C(3) 90, C(2), C(3), C(4) 110, C(1), C(2), C(3), C(4) 23, C(2), C(3), C(4), H 53, C(2), C(3), C(4), H' 207;  $a$  (= C(1), C(4)) 2.058;
- 3T<sub>M</sub>**  $C_I$  C(1), C(2) 1.487, C(2), C(3) 1.525, C(3), C(4) 1.494, C(4), C(5) 1.365, C(1), H 1.104, C(2), H 1.118, C(3), H 1.118, C(4), H 1.107, C(5), H 1.103, C(1), (2), C(3) 111, C(2), C(3), C(4) 109, C(3), C(4), C(5) 122, C(1), C(2), C(3), C(4) - 6, C(2), C(3), C(4), C(5) 33, C(3), C(4), C(5), H 197, C(3), C(4), C(5), H' 42;  $a$  (= C(1), C(5)) 2.185;
- 4T<sub>M</sub>**  $C_I$  C(1), C(2) 1.477, C(2), C(3) 1.520, C(3), C(4) 1.522, C(4), C(5) 1.490, C(5), C(6) 1.352, C(1), H 1.104, C(2), H 1.122, C(3), H 1.120, C(4), H 1.119, C(5), H 1.110, C(6), H 1.102, C(1), C(2), C(3) 119, C(2), C(3), C(4) 119, C(3), C(4), C(5) 115, C(4), C(5), C(6) 127, C(1), C(2), C(3), C(4) 40, C(2), C(3), C(4), C(5) - 39, C(3), C(4), C(5), C(6) 62, C(4), C(5), C(6), H 29, C(4), C(5), C(6), H' 188;  $a$  (= C(1), C(6)) 2.265;
- 5T<sub>M</sub>**  $C_I$  C(1), C(2) 1.473, C(2), C(3) 1.517, C(3), C(4) 1.518, C(4), C(5) 1.518, C(5), C(6) 1.490, C(6), C(7) 1.350, C(1), H 1.104, C(2), H 1.123, C(3), H 1.121, C(4), H 1.121, C(5), H 1.122, C(6), H 1.111, C(7), H 1.102, C(1), C(2), C(3) 122, C(2), C(3), C(4) 122, C(3), C(4), C(5) 122, C(4), C(5), C(6) 122, C(5), C(6), C(7) 132, C(1), C(2), C(3), C(4) 61, C(2), C(3), C(4), C(5) - 71, C(3), C(4), C(5), C(6) 47, C(4), C(5), C(6), C(7) 30, C(5), C(6), C(7), H 24, C(5), C(6), C(7), H' 182;  $a$  (= C(1), C(7)) 2.290;
- 2T<sub>S</sub>**  $C_I$  C(1), C(2) 1.496, C(2), C(3) 1.491, C(3), C(4) 1.449, C(1), H 1.112, C(2), H 1.107, C(3), H 1.109, C(4), H 1.106, C(1), C(2), C(3) 65, C(2), C(3), C(4) 117, C(1), C(2), C(3), C(4) 44; C(1)...C(3) 1.612, C(1)...C(4) 1.812;
- 3T<sub>S</sub>**  $C_I$  C(1), C(2) 1.539, C(2), C(3) 1.523, C(3), C(4) 1.513, C(4), C(5) 1.449, C(1), H 1.125, C(2), H 1.114, C(3), H 1.114, C(4), H 1.113, C(5), H 1.107, C(1), C(2), C(3) 94, C(2), C(3), C(4) 91, C(3), C(4), C(5) 126, C(1), C(2), C(3), C(4) 3, C(2), C(3), C(4), C(5) - 66; C(1)...C(4) 1.658, C(1)...C(5) 1.746;
- 4T<sub>S</sub>**  $C_I$  C(1), C(2) 1.534, C(2), C(3) 1.525, C(3), C(4) 1.525, C(4), C(5) 1.512, C(5), C(6) 1.453, C(1), H 1.136, C(2), H 1.117, C(3), H 1.117, C(4), H 1.117, C(5), H 1.114, C(6), H 1.107, C(1), C(2), C(3) 111, C(2), C(3), C(4) 109, C(3), C(4), C(5) 108, C(4), C(5), C(6) 127, C(1), C(2), C(3), C(4) 1, C(2), C(3), C(4), C(5) - 2, C(3), C(4), C(5), C(6) 75; C(1)...C(5) 1.661, C(1)...C(6) 1.692;
- 5T<sub>S</sub>**  $C_I$  C(1), C(2) 1.526, C(2), C(3) 1.520, C(3), C(4) 1.518, C(4), C(5) 1.519, C(5), C(6) 1.511, C(6), C(7) 1.455, C(1), H 1.142, C(2), H 1.119, C(3), H 1.119, C(4), H 1.119, C(5), H 1.120, C(6), H 1.117, C(7), H 1.107, C(1), C(2), C(3) 119, C(2), C(3), C(4) 118, C(3), C(4), C(5) 117, C(4), C(5), C(6) 118, C(5), C(6), C(7) 129, C(1), C(2), C(3), C(4) 37, C(2), C(3), C(4), C(5) - 41, C(3), C(4), C(5), C(6) 30, C(4), C(5), C(6), C(7) 65; C(1)...C(6) 1.653, C(1)...C(7) 1.678;

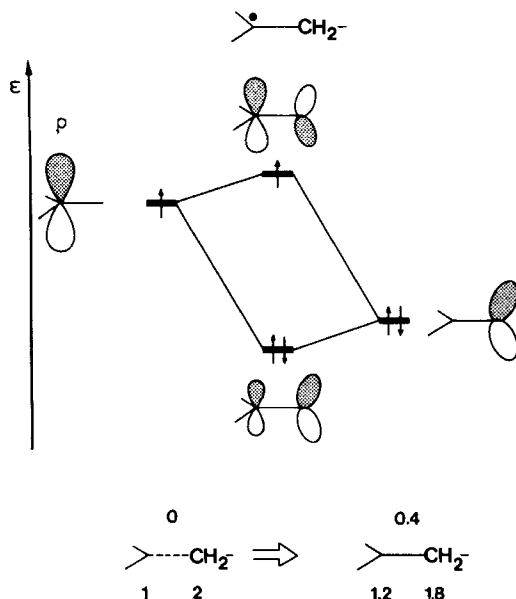


Fig.2. Qualitative interaction scheme of a singly occupied p-orbital conjugated with the pseudo p-orbital  $\sigma$  of an adjacent methylene group. The scheme given on the bottom indicates the effects upon bond orders and charge densities due to this conjugation.

The double bond moieties of the molecules show strong polarization of charge. The terminal C-atoms in all  $\omega$ -alkenyl radicals are the negative end of the local dipoles.

This polarization effect is well recognized and has been analyzed in detail by Hoffmann *et al.* [14].

Our calculations predict, that the magnitude of this polarization does not change significantly with increasing length of the substituting alkyl chain.

**Cycloalkyl radicals.** - The product expected from a cyclization of an  $\omega$ -alkenyl radical following the Markownikow route **M** is the corresponding cycloalkyl radical. The radical center of the former then has become the C-atom in  $\beta$ -position of the product radical. The calculated structures of the cyclobutyl (**2M**), cyclopentyl (**3M**), cyclohexyl (**4M**), and cycloheptyl radical (**5M**) are again summarized in Figure 3. It should be noted, that MINDO/3 is known to predict cyclic hydrocarbons too planar [15]. Although the prediction of **2M** and **3M** to possess  $C_{2v}$  symmetry therefore seems to be an artefact of the method, it is strongly supported by experimental evidence based on ESR. spectra [13 b].

As in the  $\omega$ -alkenyl radicals, the conjugation of  $p$  with adjacent  $CH_2$ - $\sigma$ -orbitals is bound to influence the structures and charge distributions accordingly: The C(1), C( $a$ )-bonds are markedly shortened, the C( $a$ ), H( $a$ )-bondlengths again longer than in the parent hydrocarbons. Although the negative charge on C(1) again is the largest in the cyclopentyl radical (**3M**), the radical center remains

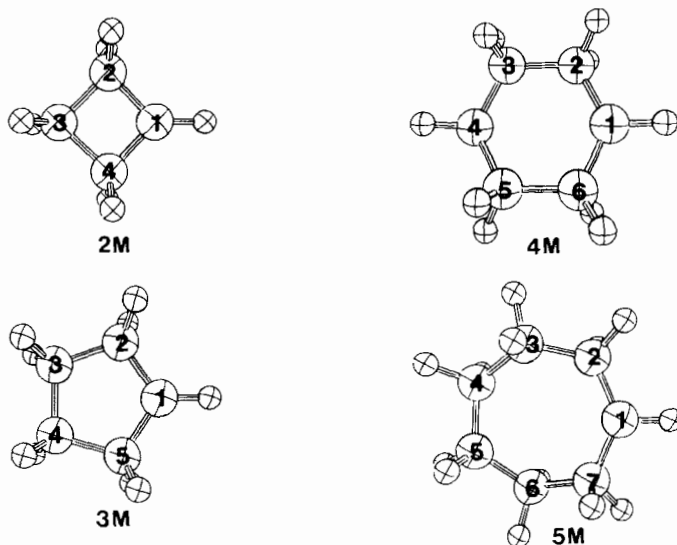


Fig.3. Calculated structures of lowest energy of cycloalkyl radicals  $nM$ . The numbering given is used to define the structural data summarized in Table 2.

planar. This is a result of the four  $H(a)$ -atoms whose repulsions force the  $H_R$ -atom into the most staggered conformation which is coplanar with the carbon skeleton.

**Cycloalkyl-methyl radicals.** - The *Anti-Markownikow* products of the cyclization of  $\omega$ -alkenyl radicals are the cyclopropyl-methyl radical (2A), the cyclobutyl-methyl-radical (3A), the cyclopentyl-methyl-radical (4A), and the cyclohexyl-methyl-radical (5A). Their structures again are shown in Figure 4.

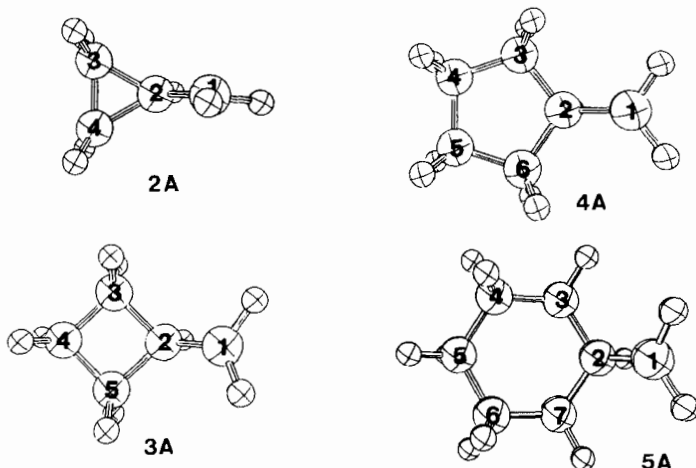


Fig.4. Calculated structures of lowest energy of cycloalkyl-methyl radicals  $nA$ . The numbering given is used to define the structural data summarized in Table 2.



Apparently, the conformation of the exocyclic methylene groups are all parallel with the ring except for **2A**, where the terminal methylene group assumes the perpendicular conformation. The reason for this behaviour is quite obvious: The singly occupied localized orbital has a much more effective partner for conjugation in **2A** than the  $\text{CH}_2$ - $\sigma$ -orbitals discussed before: The antisymmetric *Walsh* orbital [16]  $W_A$  of the cyclopropyl ring. Since the orbital energy difference between  $W_A$  and the nonbonding orbital  $\rho$  is small, the corresponding conjugation leads to a considerable gain in energy. This more than outweighs the energetic cost for one  $H_R$ -atom to be eclipsed with the adjacent  $H(a)$ -atom thus leading to the equilibrium conformation calculated for **2A**. In addition, this conjugation leads to a comparatively high rotational barrier of 7 kJ/mol for the internal rotation of the terminal methylene group, whereas the barriers calculated for **3A**, **4A**, and **5A** only amount to 1.8, 2 and 1 kJ/mol respectively. Likewise, the cyclobutyl moiety in **3A** is known to have high lying  $\sigma$ -orbitals of *Walsh* type [17]. However, the two *Walsh* orbitals  $e_A$  and  $e_S$  can both equally well interact with  $\rho$  which in turn lowers the energy of the perpendicular as well as the parallel conformation and therefore does not lead to a distinct preference of either one. Again, most recent experimental findings are in full accordance with the predicted equilibrium structures of Cycloalkyl-methyl radicals [13c].

As can be seen from these figures, the cycloalkyl-methyl radicals all possess one degree of freedom for internal rotation with very low barriers of rotation. In our calculation of entropies, they are replaced by the calculated vibrations of low frequencies as the result of the analysis of the corresponding force fields. Unfortunately, the calculated normal vibrations cannot be resolved in unique ways to yield the entropy partitions which have to be assigned to these internal rotations alone.

A further refinement of the method (such as to treat internal rotors properly) was therefore abandoned.

The discussion of reactant properties shall be concluded by a comparison of the calculated H-atom affinities  $\Delta H_H$ . These values are much better suited to compare relative stabilities of radicals than their calculated heats of formations directly. They were found by comparing the heats of formation of the radicals  $R\cdot$  with those of the associated parent hydrocarbons  $RH$  in their predicted equilibrium structures and are formally the adiabatic heats of reaction shown below. Note, that their absolute values are most likely too low by about 40 kJ/mol for the reasons given in [3].



$$\begin{aligned} \Delta H_H(R\cdot) &= \Delta H_f(R\cdot) + \Delta H_f(H\cdot) - \Delta H_f(RH) \\ &= \Delta H_f(R\cdot) - \Delta H_f(RH) + 218 \text{ kJ/mol} \end{aligned}$$

The results have been given in *Table 1*. Apparently, the  $\Delta H_H$  values calculated for the  $\omega$ -alkenyl radicals do not change with increasing length of the C, C-chain. They are approximately identical with those found for the saturated alkyl-radicals [3]. On the other hand, **2A** and **3A** show  $\Delta H_H$  values which are considerably

lower than those of the higher homologues. This again can be understood in terms of stabilization of the radical by interaction with the *Walsh* orbitals as outlined above.

The most pronounced trend in  $\Delta H_H$ , however, is predicted in the series of the cycloalkyl radicals **nM** and has the opposite direction. Although the thermocycle calculations using experimental values [3] corroborate this result for small rings in the series, the resulting trend using the calculated heats of formation is probably exaggerated.

Finally, it should be noted, that the relative stability of the radicals **n**, **nA**, and **nM** turns out to be



for all systems except for  $n=2$ , in which the ring strain of the three membered ring reverses the ordering of **n** and **nA** thus making the homoallyl radical **2** to be more stable than the cyclized cyclopropyl-methyl radical **2A**. This is consistent with experimental findings [18] and *ab initio* calculations using the extended basic set STO 4-31 G [19].

**Reaction pathways.** - We shall now discuss the possible reaction pathways interconnecting the three minima on each potential surface which we have represented in the paragraphs above.

The energetics controlling the outcome of such rearrangements can be predicted by computing the structures and properties of the associated saddle points according to *Eyring's* theory of the activated complex [20]. Such structure determinations can in principle be carried out by optimizing the gradient square  $\sigma$  as developed by *McIver & Komornicky* [21]. Our experience with this method, however, was frustrating, because a dependable way to calculate the necessary second derivative must be carried out using a mesh of points each calculated by a full SCF calculation<sup>4</sup>). We therefore turned to the alternative method of locating saddle points given in the appendix A.

Three possible reaction pathways on each potential surface have been investigated (see *Scheme*):

- a) The *Markownikow* cyclization of  $\omega$ -alkenyl radicals (route **M**);
- b) the alternative *Anti-Markownikow* cyclization (route **A**) and
- c) a possible direct rearrangement of the cyclic radicals *via* a synchronous 1,2-alkyl shift (route **S**).

The calculated thermodynamical data are collected in *Table 3*, the obtained structures of the associated saddle points shown in *Figure 5*. The arrows shown in the figure represent the nuclear displacements along the intrinsic reaction coordinate [23] or transition vector [24] calculated [25] for the individual saddle points.

From the values given in *Table 3* there are four trends readily apparent:  
With increasing  $n$ ,

- a) the activation energy of route **M** decreases

<sup>4</sup>) Unlike in the computation of first derivatives, the changes in the bondorder matrices (*i.e.* wavefunction forces) can no longer be neglected for the second derivatives. See also [22].

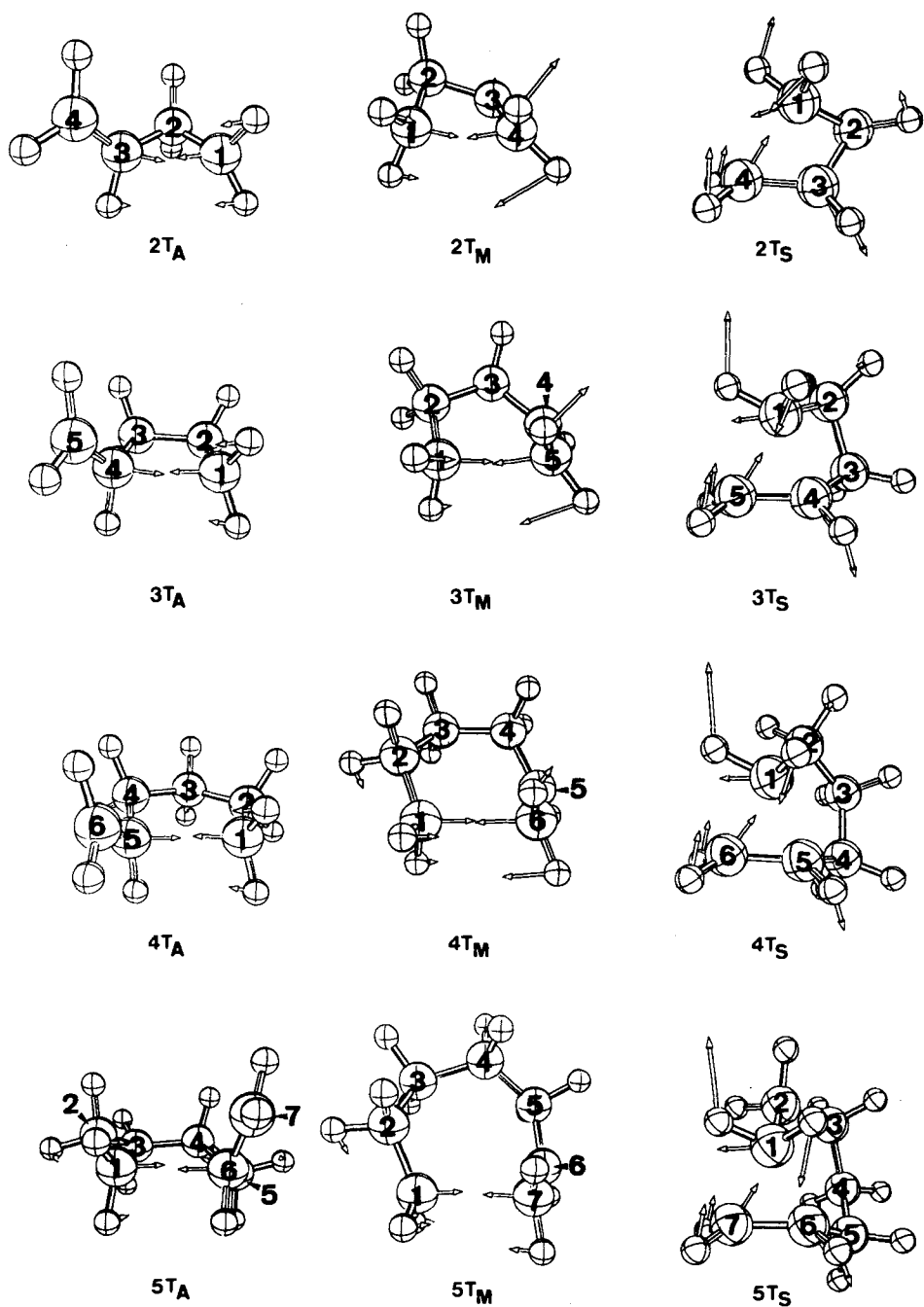


Fig.5. Calculated structures of activated complexes  $nT_A$ ,  $nT_M$  and  $nT_S$  corresponding to the three investigated reaction pathways. The arrows indicate the nuclear displacements along the intrinsic reaction coordinates.

Table 3. Activation energies ( $\Delta H^\ddagger$ ), activation entropies ( $\Delta S_{298}^\ddagger$ ), and free activation energies ( $\Delta G_{298}^\ddagger$ ) of the three possible rearrangement processes **M**, **A** and **S** specified in the text. All values in kJ/mol and J/K mol respectively.

n	Route M			Route A			Route S		
	$\Delta H^\ddagger$	$\Delta S_{298}^\ddagger$	$\Delta G_{298}^\ddagger$	$\Delta H^\ddagger$	$\Delta S_{298}^\ddagger$	$\Delta G_{298}^\ddagger$	$\Delta H^\ddagger$	$\Delta S_{298}^\ddagger$	$\Delta G_{298}^\ddagger$
2	123	-40	135	52	-34	62	135	-16	140
3	93	-51	108	77	-48	91	139	-22	145
4	69	-69	89	69	-55	85	136	-22	142
5	67	-80	91	79	-80	103	136	-19	142

b) the activation energy of route **A** (except for  $n=3$ ; see below) generally increases,

c) the activation entropies of both cyclization mechanisms become more and more negative while

d) the activation energy as well as activation entropy of route **S** remain about constant.

These trends predicted by our MINDO/3 calculations nicely reflect the observed characteristics of the series and lead to conclusions which are equally reasonable and illustrative.

Nevertheless, we must admit, that the calculated activation parameters *quantitatively* compare poorly with experimental findings: All values are too large in magnitude [13] [26]. The reason for this might be due to correlation effects which are not taken care of properly in a one configuration model such as MINDO/3-UHF. Most likely, these effects have a bigger influence on activated complexes than on equilibrium structures which on the other hand make the single determinant activation energies turn out too high. We believe, that the use of an appropriate model would be extremely expensive and the additional information it might yield would not pay out.

Table 3 shows as expected, that the limiting factor to observe cyclization is due to entropy: The intramolecular attack of the radical at the double bond becomes more and more unlikely - the activation entropy becomes too negative as  $n$  gets large.

For all systems studied, the activation energy for a 1,2-alkyl shift (route **S**) is much larger and does not offer a competitive course to form the thermodynamically more stable product  $n\mathbf{M}$  by a two step reaction  $n \rightarrow n\mathbf{A} \rightarrow n\mathbf{M}$ . Our method predicts, that if the cycloalkyl radical is formed at all (as in the case of the  $\omega$ -hexenyl radical [27] and the higher homologues [28]), a conversion of the cycloalkyl-methyl radical must involve the corresponding  $\omega$ -alkenyl radical. This is in full accordance with experiment [29].

At first sight the most surprising trends are a) and b) mentioned above. They deserve further comment because they explain very clearly the observed experimental data. Comparing the calculated free activation enthalpies  $\Delta G_{298}^\ddagger$  (which in turn determine the relative rates of reaction) shows, that for small  $n$  route **A** dominates the cyclization, whereas in case of the  $\omega$ -hexenyl radical ( $n=4$ ) route **M** becomes competitive and finally controls the situation for larger systems. In other

words: Any larger  $\omega$ -alkenyl radical should behave 'normal' and cyclize to the thermodynamically more stable cycloalkyl radical just as in bimolecular radical additions [30].

There is just one number which does not fit into the scheme: The activation enthalpy for the route **A** cyclization of  $\omega$ -pentenyl radical is much larger than expected. The energy partitioning analyses traces the cause for this behaviour to a strongly antibonding transannular interaction between the methylene groups 1,3 and 2,4 of the four-membered ring in the activated complex. No such interactions are of significance in any other activated complex of the series. Although the activation entropy is on line with the other route **A** cyclizations, it makes this reaction to become much slower than both the higher and the lower homologue cyclizations. In fact, this reaction has not been observed experimentally [8]. The most pronounced trend is definitely predicted in the activation enthalpies of route **M**. The obtained results for the route **A** activation enthalpies refute the naive expectation, that this effect might be due to just the diminishing ring strain in the activated complexes.

The predicted main cause can be deduced from *Figure 5*, where the structures of the activated complexes have to be compared. The intrinsic reaction coordinates in route **A** saddle points indicate smooth bond formation and resemble pure C,C-stretch vibrations. The IRC's of route **M** saddle points on the other hand are much more complex and are strongly coupled with a torsional vibration decoupling the terminal double bond of the  $\omega$ -alkenyl radical.

Such a decoupling is bound to raise the energy of the molecule the more, the larger the decoupling angle  $\alpha$  becomes.

If we define the torsional angle  $\alpha$  as the dihedral angle between the lobes of the p-orbitals perpendicular on the planes of the substituents,  $\alpha$  amounts to  $28^\circ$  for  $n=2$ ,  $18^\circ$  for  $n=3$ ,  $9^\circ$  for  $n=4$  and  $5^\circ$  for  $n=5$ . In a simple perturbational picture, the associated raise in energy  $\Delta E$  can be estimated if the following proportionality is assumed<sup>5)</sup>:

$$\Delta E = k(1 - \cos \alpha)$$

The proportionality constant  $k$  is given by the experimentally assigned value of 260 kJ/mol for the complete decoupling of ethylene [31].

In this model, the expected decoupling energies  $\Delta E$  amount to 31 kJ/mol for  $n=2$ , 13 kJ/mol for  $n=3$ , 4 kJ/mol for  $n=4$  and is negligible for any higher member of the series. Comparing these values with those of *Table 3* reveals, that this effect indeed makes up for the major part of the calculated trend for the route **M** activation enthalpies.

This decoupling effect is due to the geometrical constraint which becomes smaller as  $n$  increases, because the radical gains more dynamic freedom to approach the double bond in a better way.

As already anticipated, the expected rate of reaction is not only a function of its activation enthalpy  $\Delta H^\ddagger$  but of the associated loss of entropy  $\Delta S_{298}^\ddagger$  to form

<sup>5)</sup> This proportionality follows, if the  $\Pi/\Pi^*$ -split is taken to be proportional to the p/p overlap integral.

the activated complex as well. This will be of greatest importance, if two competing reactions have comparable activation enthalpies as predicted for the two cyclization mechanisms of  $\omega$ -hexenyl radical (**4**) and the higher homologues. Such reactions are expected to be very sensitive to small steric and electronic changes. Experimental evidence strongly supports this expectation for a large series of derivatives of **4** [27] [32].

We wish to conclude this paragraph by briefly summarizing the outlined results:

1) The decoupling effect of the terminal double bonds hinders the small  $\omega$ -alkenyl radicals to form the thermodynamically more stable *Markownikow* products. Hence, the reaction path is not governed by the stability of the product;

2) This trend is supported by the charge distribution in the open chain reactant, because the negatively charged radical center is more likely to attack the positively polarized C-atom of the double bond;

3) A further support is given by the larger entropy of route **A** activated complexes as compared with route **M** activated complexes due to one degree of freedom for internal rotation of the former;

4) For larger systems, the dominant effect 1) has been diminished and the cyclization is governed by the same electronic effects [9] which are responsible for the *Markownikow* selectivity of bimolecular radical additions [11].

Since the third effect can only roughly be estimated in our procedure, and because such effects are rather critical if the activation enthalpies do not differ much (as for  $n > 4$ ), the switch calculated for the activation enthalpies ( $n = 4$ ) is not conclusive for the relative rates of reactions.

An entirely different point of view is reached, if the series is extended to the smallest possible system: *i.e.* What happens for  $n = 1$ ? In this case, the corresponding  $\omega$ -alkenyl radical turns into an allyl system where the radical center is formally not conjugated with the double bond, **1A** likewise becomes the allyl radical and **1M** the cyclopropyl radical.

Formulating the three possible reaction pathways accordingly, it turns out, that route **A** is a simple rotation around the C, C-single bond (leading to the 'two membered' ring), while route **M** and route **S** become the classical cases of forbidden radical rearrangement reactions: the allyl/cyclopropyl rearrangement [33].

This extension was initiated by the appearance of the activated complex of the route-**M** cyclization of the  $\omega$ -butenyl radical, where the structure as well the transition vector are very similar to the corresponding ones found for the forbidden rearrangement mentioned above ( $n = 1$ ) [1] [34].

Hence, the three reaction pathways for  $n = 1$  are in fact the lower ends of the series showing the correct extremes of activation parameters.

This extension, which in the backward glance is trivial, has to our knowledge never been made so far and provides a useful key to understanding: Updating the values given in *Table 3* thus leads to the plot shown in *Figure 6* which turns the formerly unexpected outcome of cyclization mechanisms into the most natural, well understood sequence.

The 'real'  $\omega$ -alkenyl radical cyclizations ( $n > 1$ ) which have been outlined above in this view become individual probes along an interesting series: For

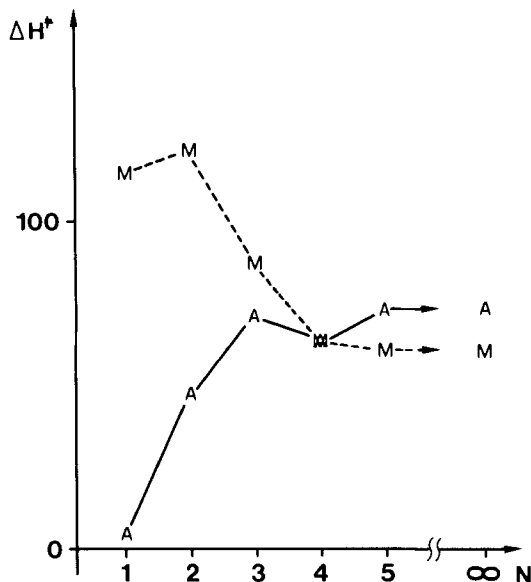


Fig. 6. Schematic representation of calculated activation enthalpies  $\Delta H^\ddagger$  as a function of increasing number of methylene groups for route **A** (solid line) and route **M** (broken line) cyclizations. (The values for  $n=1$  have been taken from [35]).

$n=1$ , route **M** is (as an interconversion between lumomers [35]) forbidden while route **A** is not, for  $n=\infty$  the 'cyclization' is a bimolecular radical addition known to proceed along the alternative route **M**.

The author is grateful to Prof. C. Rüchardt who initiated the presented study by a motivating discussion. The computations were carried out at the 'Rechenzentrum der TH Darmstadt' and the generous gift of computer-time is acknowledged.

#### Appendix A. Location and Verification of Activated Complexes.

For the reasons given in the preceding text, we switched to the old-fashioned step search commonly applied by many authors. Since the verification we used seems to be more rigid than in previous work, we wish to describe the full procedure.

Minima on the potential energy surface  $E$  in most cases represent structures which can be described by classical *Kekulé* formula. This in turn serves as a useful guide to make a good starting point choice. However, such chemical intuition does not help much in estimating the structure of an activated complex. In other words: It is hard to estimate the length of a 'dotted' chemical bond. It is the length of this bond which in most cases changes its value the most as the reactant structure continuously turns into that of the product along the reactionpath.

This length  $a$  was therefore chosen as a trial reaction coordinate. In principle, the search may start from either side of the reaction scale. Both ways should

lead to the same saddle point provided that no intermediate gives rise to a two step reaction.

Our experience taught us to start from that side on which the bond is formed and increase the value of  $a$  stepwise, optimizing the remaining  $3N-7$  variables. Once the suspected saddle point was reached (where  $dE/da=0$ ), the normal coordinates or principal directions  $|q\rangle$  were calculated by the standard procedure [25].

We found it necessary to calculate the first derivatives with respect to all principal directions  $|q\rangle$  by finite differences, making sure that they were all below the convergence criteria. This was done for all  $3N-6$  principal directions, including the transition vector  $|q_1\rangle$ , the only one, for which the obtained eigenvalue is negative.

The structure  $|t\rangle$  of the saddle point was then modified by the transition vector  $|q_1\rangle$  which led to two nearly identical structures  $|t\rangle^+$  and  $|t\rangle^-$  as

$$|t\rangle^+ = |t\rangle + \lambda |q_1\rangle$$

and

$$|t\rangle^- = |t\rangle - \lambda |q_1\rangle.$$

The scalar  $\lambda$  was chosen as 0.01. The two structures  $|t\rangle^+$  and  $|t\rangle^-$  were then fully optimized and converged to the 'end points' of the elementary reaction step.

However, in most cases, the obtained structures did not correspond to the lowest minimum of the rotamer manifold of  $\omega$ -alkenyl radicals but rather to the local minimum 'closest' to the starting structure ( $|t\rangle^+$ ) as anticipated in the preceding paragraph.

#### **Appendix B. Estimating Standard Entropies of Radicals.**

Standard entropies of molecules can be calculated by means of statistical thermodynamics [12]. The partitions which add up to the resulting standard entropy  $S_{298}^0$  contribute as:

$$S_{298}^0 = S_{tr}^0 + S_{rot}^0 + S_{irot}^0 + S_{vib}^0 + S_{el}^0$$

in the order of their approximate magnitudes.

Since in the calculation based on the  $3N-6$  dimensional forcefield the contributions of internal rotors  $S_{irot}^0$  are obviously replaced by contributions of torsional vibrations of very low frequencies, the method is bound to fail, if this replacement becomes exhaustive. Standard entropies of systems such as the  $\omega$ -alkenyl radicals can therefore not be calculated by this treatment.

Inspection of the measured standard entropies of linear alkanes reveals, that the lengthening of the chain by one methylene group consistently raises the standard entropy of the molecule by 40 J/Kmol [36]. We therefore calculated the standard entropy of the smallest member of the series (2), adding 40 J/Kmol to each next higher homologue.



## BIBLIOGRAPHY

- [1] *M. J. S. Dewar*, *Chem. in Britain* 11, 97 (1975).  
[2] *R. C. Bingham, M. J. S. Dewar & D. H. Lo*, *J. Am. Chem. Soc.* 97, 1285 (1975).  
[3] *P. Bischof*, *J. Am. Chem. Soc.* 98, 6844 (1976).  
[4] *P. Bischof*, *J. Am. Chem. Soc.* 99, 8145 (1977).  
[5] *M. J. S. Dewar & S. Olivella*, *J. Am. Chem. Soc.* 100, 5290 (1978).  
[6] *M. J. S. Dewar & S. Olivella*, *J. Am. Chem. Soc.* 101, 4958 (1979).  
[7] *E. Haselbach, T. Bally & Z. Lanyiova*, *Helv.* 62, 577 (1979) and references cited therein.  
[8] *P. Bischof*, *Tetrahedron Lett.* 1979, 1291.  
[9] *J. Franklin, J. D. Dillard, H. M. Rosenstock, Y. T. Herron, K. Draxl & F. M. Field*, *Natl. Stand. Ref. Data Ser., Nat. Bur. Stand., No. 26* (1969) and experimental references in ref. [3].  
[10] *J. M. Tedder & J. C. Walton*, *Tetrahedron* 36, 701 (1980).  
[11] *V. Bonacic-Koutecký, J. Koutecký & L. Salem*, *J. Am. Chem. Soc.* 99, 842 (1977).  
[12] *I. N. Godnew*, «Berechnungen thermodynamischer Funktionen aus Moleküldaten», Deutscher Verlag der Wissenschaften, Berlin 1963.  
[13] *Landolt-Börnstein*, Neue Serie, Gruppe II, Vol. 9b (1978); *H. Fischer*, 'Structure of Free Radicals by ESR Spectroscopy' in 'Free Radicals', Vol. II, ed. by *J. K. Kochi*, *J. Wiley & Sons*, New York (1973) and references cited therein, specifically: a) *D. J. Edge & J. K. Kochi*, *J. Am. Chem. Soc.* 94, 7695, (1972); b) *T. Ohmae, S. Ohnishi, K. Kuwata, H. Sakurai & I. Nitta*, *Bull. Chem. Soc. Japan* 40, 226 (1967); c) *P. M. Blum, A. G. Davies & R. A. Henderson*, *Chem. Comm.* 1978, 569.  
[14] *L. Libit & R. Hoffmann*, *J. Am. Chem. Soc.* 96, 1370 (1974).  
[15] *R. C. Bingham, M. J. S. Dewar & D. H. Lo*, *J. Am. Chem. Soc.* 97, 1294 (1975).  
[16] *A. D. Walsh*, *Nature* 159, 167, 712 (1947).  
[17] *P. Bischof, E. Haselbach & E. Heilbronner*, *Angew. Chem.* 82, 952 (1970); *R. Gleiter, P. Bischof, W. E. Volz & L. A. Paquette*, *J. Am. Chem. Soc.* 99, 8 (1977) and references therein.  
[18] *A. L. J. Beckwith*, 'Essays on Free Radical Chem.' *Spec. Public.* 24, 239 (1970).  
[19] *W. J. Hehre*, *J. Am. Chem. Soc.* 95, 2643 (1973).  
[20] *H. Eyring*, *J. Chem. Phys.* 3, 107 (1935).  
[21] *J. W. McIver & A. Komornicky*, *J. Am. Chem. Soc.* 94, 2625 (1972).  
[22] *P. Pulay*, *Mol. Phys.* 17, 197 (1969).  
[23] *K. Fukui, S. Kato & H. Fujimoto*, *J. Am. Chem. Soc.* 97, 1 (1975).  
[24] *A. Komornicky & J. W. McIver Jr.*, *J. Am. Chem. Soc.* 98, 4553 (1976).  
[25] *M. J. S. Dewar & G. P. Ford*, *J. Am. Chem. Soc.* 99, 1685 (1977).  
[26] *P. Schmid, D. Griller & K. U. Ingold*, *Int. J. Chem. Kinet.* 11, 333 (1979); *A. Effio, D. Griller, K. U. Ingold, A. L. J. Beckwith & A. K. Serelis*, *J. Am. Chem. Soc.* 102, 1733 (1980).  
[27] *C. Walling & A. Cioffari*, *J. Am. Chem. Soc.* 94, 6059 (1972).  
[28] *C. Walling & A. Cioffari*, *J. Am. Chem. Soc.* 94, 6064 (1972).  
[29] *J. W. Wilt*, 'Free Radical Rearrangements', p.340 in 'Free Radicals', Vol. 1, ed. by *J. K. Kochi*, *J. Wiley & Sons*, New York 1973.  
[30] *B. Giese & J. Meixner*, *Tetrahedron Lett.* 1977, 2279.  
[31] *M. H. Wood*, *Chem. Phys. Lett.* 24, 239 (1974).  
[32] *M. Julia*, *Pure Appl. Chem.* 15, 167 (1967); *M. Julia*, *Acc. Chem. Res.* 4, 386 (1971); *C. Walling, J. H. Cooley, A. A. Ponaras & E. J. Racah*, *J. Am. Chem. Soc.* 88, 5361 (1966) and references therein.  
[33] *H. C. Longuet-Higgins & E. W. Abrahamson*, *J. Am. Chem. Soc.* 87, 2045 (1965).  
[34] *P. Bischof & G. Friedrich*, to be published.  
[35] *M. J. S. Dewar, S. Kirschner & H. Kollmar*, *J. Am. Chem. Soc.* 96, 5240 (1974).  
[36] JANAF (United States Joint Army, Navy, Air Force), *Interim Thermochemical Tables*, Vols. 1 and 2, Thermal Laboratory, The Dow Chemical Company, Midland, Michigan 1965.